

# Q-space Velocimetry Methods Applied to Flowing Hyperpolarized Xenon

W. Barros<sup>1</sup>, R. W. Mair<sup>1</sup>, M. S. Rosen<sup>1,2</sup>, and R. L. Walsworth<sup>1,2</sup>

<sup>1</sup>Harvard-Smithsonian Center for Astrophysics, Cambridge, MA, United States, <sup>2</sup>Dept. of Physics, Harvard University, Cambridge, MA, United States

**Introduction:** There has been recent interest in the use of MR velocimetry techniques to study flow of hyperpolarized noble gases with the aim of elucidating flow patterns in human airways during inhalation [1-4], although only a couple of *in-vivo* results have been presented [1,4]. However, all these studies use the phase-contrast (PC) velocimetry method where velocity in a pixel is determined from the signal phase variation with the addition of one flow-encoding gradient [5]. The Fourier-encoding (**q**-space) velocimetry method has been used for some time in the non-medical MRI community [6,7], which provides a wealth of additional data that is useful in characterizing non-stationary flows. Fourier-inversion of the NMR signal attenuation as a function of parameters related to flow-encoding gradient strength, for multiple values of this gradient, yields an image of the velocity spectrum for spins in the region of interest [6], rather than a single value of velocity. In addition, the use of a double-PGSE method [8] allows the discrimination between coherent flow and velocity fluctuations, as well as between Brownian self-diffusion and enhanced dispersion that occurs due to shearing across velocity streamlines. In this study, we examine the full velocity spectrum obtained from the **q**-space velocimetry technique, and the use of the double-PGSE technique in gas flow for the first time.

**Methods:** All measurements were made on hyperpolarized xenon gas flowing through a 6 mm ID tube in a 4.7 T vertical-bore NMR magnet. <sup>129</sup>Xe spins in a gas mixture of ~ 92% xenon/8% N<sub>2</sub> were hyperpolarized by spin-exchange optical pumping using a novel line-narrowed 30 W diode-array laser [9]. The polarizer operated in a continuous flow mode, with gas flowing constantly from the gas bottle, through the optical pumping cell, and on to the tubing inside the magnet under the influence of a vacuum pump, with flow rates moderated by a mass flow controller between the magnet and pump [10]. The NMR system was a Bruker DMX-200-based system with micro-imaging gradient capability, and employed a homebuilt saddle-coil tuned to 55.4 MHz. **q**-space velocimetry and double-PGSE experiments were performed without slice selection, either spectroscopically or with 1D spatial localization. For all experiments,  $\delta = 1$  ms,  $\Delta = 10$  ms,  $g$  varied from 0 to 35.7 G/cm, and  $\tau$  in the double-PGSE experiment = 5 ms.

**Results:** Figure 1 shows 1D velocimetry profiles for xenon gas flow at two different flow rates. The “image” shows a velocity spectrum for each position across the cross-section of the tube [11]. The most predominant velocity (ie, the value given by the PC-MRI method) in each pixel is given by the darkest red color. At low flows, there is little variation in the most predominant velocity, the velocity spectrum is very narrow, and the maximum in the probability distribution of velocities is the same in each pixel. At the higher flow rate, velocity shearing begins to occur as spins cross velocity streamlines. The velocity spectrum broadens in the middle of the tube, but there is little change at the edges. The effect of velocity shear, or dispersion, is also seen in the comparison between single- and double-PGSE spectroscopic measurements in Fig. 2. At low flow, both experiments exhibit a linear decay of  $\ln(S/S_0)$  vs  $q^2$ . The double-PGSE data decays at twice the rate of the single-PGSE data, as twice as much diffusion-encoding is applied. However, at high flows, the apparent diffusion, as measured by the single-PGSE experiment, is enhanced dramatically by dispersion effects, while the double-PGSE data is mostly unchanged.

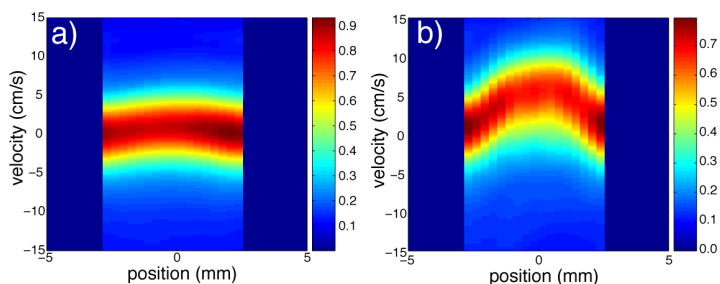


**Fig. 1:** 1D flow profiles of xenon gas flowing through a 6 mm ID tube for flow rates of 50 (a) and 180 (b) sccm. Areas outside the tube have been zeroed. The colors indicate the probability distribution of velocities for spins flowing at a given spatial profile location; i.e. each column is a velocity spectrum for that profile position.

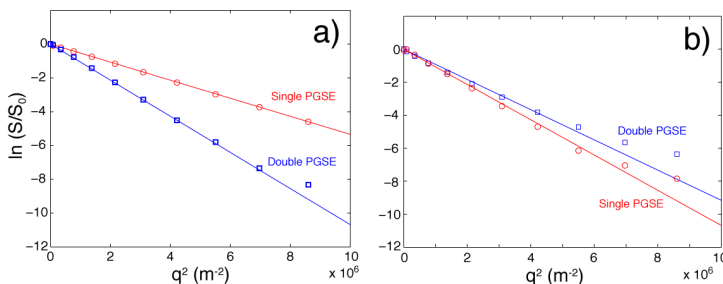


**Fig. 2:** Signal attenuation plots obtained using single- and double-PGSE spectroscopic methods for xenon gas flowing through a 6 mm ID tube for flow rates of 50 (a) and 180 (b) sccm.  $q = \gamma \delta g / 2\pi = 1/\text{wavelength}$  for  $2\pi$  dephasing of spins due to a given gradient strength [5].

**Discussion:** The flow velocimetry image data was verified by calculating the overall flow velocity for gas in a tube, based on the tube diameter and flow rate set at the mass flow controller. As expected for laminar flow, the (most predominant) maximum velocity observed is ~ half that of the overall velocity [11]. For non-coherent or turbulent flows, and high flow rates with excessive velocity-shearing, the velocity spectrum provides additional useful information to understand the flow field that is not available from the PC-MRI method. The full velocity spectrum obtained with complete 2D spatial resolution, and similar data using double-PGSE encoding, will provide a powerful tool for better studying gas flow and velocity fluctuations in lung models, as it has in materials science previously [12].

**Acknowledgements:** This work was supported by the NSF under grant numbers PHY-0618891 and CBET-0651628.

## References

1. L. de Rochefort et al, *Magn. Reson. Med.*, **55**, 1318 (2006).
2. W. Killian et al, *Proc. 15<sup>th</sup> ISMRM*, 1278 (2007).
3. J.M. Woodburn et al, *Proc. 15<sup>th</sup> ISMRM*, 1277 (2007).
4. K.R. Minard et al, *J. Magn. Reson.*, **194**, 182 (2008).
5. P.R. Moran, *Magn. Reson. Imaging*, **1**, 197 (1983).
6. P.T. Callaghan, *Principles of NMR Microscopy*, OUP (1991).
7. R.W. Mair et al, *Magn. Reson. Chem.*, **40**, S29 (2002).
8. P.T. Callaghan et al, *Concepts Magn. Reson.*, **11**, 181 (1999).
9. R.W. Mair et al, *Magn. Reson. Imaging*, **25**, 549 (2007).
10. T. Pavlin et al, *Appl. Magn. Reson.*, **32**, 93 (2007).
11. L.G. Kaiser et al, *J. Magn. Reson.*, **149**, 144 (2001).
12. J.D. Seymour et al, *Phys. Rev. Lett.*, **84**, 266 (2000).